USCAP

ARTICLE

LncRNA GAS5 regulates migration and epithelial-to-mesenchymal transition in lens epithelial cells via the miR-204-3p/*TGFBR1* axis

Xiao Li[1], Miaomiao Sun[1], Anran Cheng[1] and Guangying Zheng[1]✉

Diabetic cataract (DC) is a major ocular complication secondary to diabetes mellitus. The epithelial-mesenchymal transition (EMT) of lens epithelial cells (LECs) is an important event in DC progression. Long non-coding RNAs (lncRNAs) and microRNAs are involved in various biological processes and disorders. The aim of this study was to investigate the roles of lncRNA growth arrest-specific transcript 5 (GAS5) and microRNA-204-3p (miR-204-3p) deregulation in the pathogenic mechanism of high glucose (HG)-stimulated LECs. The results show that GAS5 was up-regulated, whereas miR-204-3p was down-regulated in anterior lens capsule tissues of DC patients and in HG-treated LECs compared to their controls, respectively. Functional experiments suggest that the lentivirus-mediated depletion of GAS5, as well as overexpression of miR-204-3p, suppressed migration and EMT in HG-treated LECs. Further mechanistic studies revealed that lncRNA GAS5/miR-204-3p/type 1 receptor of transforming growth factor-beta (*TGFBR1*) has a regulatory role in the process. Collectively, we demonstrated that dysregulation of GAS5 affects lens epithelial cell migration and EMT under HG conditions via the miR-204-3p/*TGFBR1* axis. The current findings may provide new insights into the molecular mechanisms of DC development.

Laboratory Investigation (2022) 102:452–460; https://doi.org/10.1038/s41374-021-00713-3

INTRODUCTION

Cataracts rank first among eye diseases causing blindness worldwide, largely resulting from aging and diabetes mellitus[1]. Patients with diabetes mellitus have an increased incidence of cataracts, characterized by early-onset age, rapid progression of lens opacity, and quick maturation[2]. Epidemiological studies have revealed that populations with diabetic cataract (DC) is of 5-fold higher prevalence[3,4], and the cataractogenesis process is accelerated by 20-years compared to nondiabetic counterparts[5]. To date, surgical treatment is the only effective strategy for treating DC. However, it frequently leads to complications and is costly, which brings a heavy burden on the medical systems[6]. It is therefore of great importance to explore the molecular mechanisms underlying the pathogenesis of DC.

Normal growth of eye lens involves systematic proliferation of lens epithelial cells (LECs) and their subsequent differentiation into fiber cells, which is essential for lens transparency[7]. However, under high glucose (HG) conditions, LECs undergo epithelial-to-mesenchymal transition (EMT) and develop characteristics of mesenchymal cells such as high migratory capacity and invasiveness, which are the foundational basis for DC occurrence and development[8,9]. Recent studies support the hypothesis that DC is closely associated with EMT of LECs[10,11]. Revealing the mechanism involved in the HG-induced high migration and EMT of LECs is vital to understand the pathology of DC.

It is estimated that 98% of the human genome transcripts are non-coding RNAs (ncRNAs), which participate in the regulation of cellular bioprocesses and disorders[12]. Long non-coding RNAs (lncRNAs) are a group of ncRNAs over 200 nucleotide (nt) length, and have been confirmed to modulate various biological processes at epigenetic, transcriptional, and post-transcriptional levels or directly regulate protein activity[13]. Certain lncRNAs, including metastasis-associated lung adenocarcinoma transcript 1 (MALAT1), plasmacytoma variant translocation 1 (PVT1), and nuclear enriched abundant transcript 1 (NEAT1), are important regulators in DC development[14–16]. Notably, lncRNA growth arrest-specific transcript 5 (GAS5) is originally isolated from murine NIH 3T3 cells and acts as a potential tumor suppressor in multiple malignancies[17]. Silencing of GAS5 alleviates HG toxicity to human renal tubular epithelial cells[18]. Also, repression of GAS5 relieves glaucoma symptoms in rats by impeding retinal ganglion cell apoptosis[19]. Nevertheless, the function of GAS5 in DC remains unknown.

There is evidence suggesting the participation of mRNA-miRNA-lncRNA network in multiple human diseases. Several studies showed that miRNAs (miR-30a, miR-199a-5p, and miR-211) might serve as potential biomarkers or novel therapeutic targets for DC.[9,10,20]. Using bioinformatics, we identified miR-204-3p as a potential target miRNA of lncRNA GAS5. Knockdown of lncRNA AK139328 relieves myocardial ischemia/reperfusion injury and inhibits cardiomyocyte autophagy in diabetic mice via modulating miR-204-3p[21]. Moreover, Wu et al. reported that miR-204-3p expression was down-regulated in cataract lenses and was found to target 3′ UTR of pro-oxidative genes[22], which indicates that miR-204-3p may be involved in cataract development.

[1]Department of Ophthalmology, The First Affiliated Hospital of Zhengzhou University, No. 1 Jianshe East Road, Zhengzhou 450000 Henan, China. ✉email: zzzgy@zzu.edu.cn

Received: 18 June 2021 Revised: 15 November 2021 Accepted: 19 November 2021
Published online: 16 December 2021

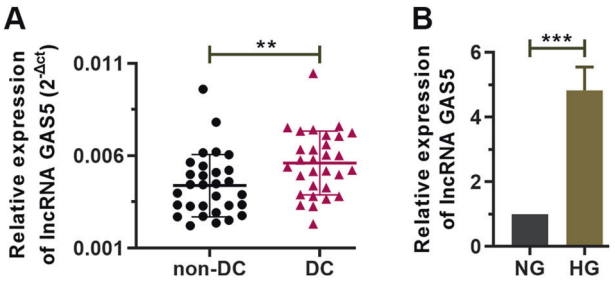

Fig. 1 The expression of lncRNA GAS5 is enhanced in the anterior lens capsules of DC patients and in HG-treated LECs. A The expression of lncRNA GAS5 was detected using real-time PCR in the anterior lens capsules of non-DC ($n = 30$) and DC ($n = 30$) patients. **B** The expression of lncRNA GAS5 was detected using real-time PCR in NG or HG-treated LECs ($n = 3$, each group). Data are presented as the mean ± SD. $^{**}P < 0.001$, $^{***}P < 0.001$, compared with non-DC group or NG group.

Nevertheless, its role in DC also remains unclear. We also found that the type 1 receptor of transforming growth factor-beta (*TGFBR1*), a key receptor of the TGF-β/Smad signaling path[23] way, is a potential target gene of miR-204-3p. TGF-β/Smad signaling is widely accepted as a key inducer of EMT of LECs[23–26]. Herein, we systematically evaluated the regulative roles of lncRNA GAS5/miR-204-3p/*TGFBR1* axis in an HG-stimulated LEC model.

MATERIALS AND METHODS

Collection of clinical samples

After receiving a full explanation about the surgical procedures and possible complications, informed consent were written by all patients enrolled in this study. Fresh anterior lens capsules were obtained from patients diagnosed with age-related cataract (ARC) with or without type 2 diabetes mellitus (T2DM) and underwent phacoemulsification & intraocular lens implantation in the First Affiliated Hospital of Zhengzhou University between January 2020 and December 2020. Inclusion criteria for patients with cataract were based on clinically observable grade III cortical cataracts according to the Lens Opacities Classification System III with or without T2DM, whereas the ones with a history of ocular surgery, high myopia, diabetic retinopathy, eye trauma, glaucoma or shallow anterior chamber, optic neuropathy or other fundus diseases were excluded. T2DM patients hereby indicated the ones with typical diabetic manifestations (polyuria, polydipsia, and inexplicable weight loss) and with one of the following characteristics: 1) Fasting blood glucose levels over 7 mmol/L; 2) Blood glucose levels over 11.1 mmol/L following 2 h oral glucose tolerance test; 3) Random blood glucose levels over 11.1 mmol/L. A total of 30 patients with DC and 30 patients with non-DC were adopted in the study. The average T2DM duration of DC patients was 15.32 ± 4.17 years.

Cell culture

Human LECs and 293 T cells were purchased from Zhong Qiao Xin Zhou Biotechnology Co., Ltd. (Shanghai, China). LECs were cultured in an epithelial cell culture medium (ScienCell, San Diego, CA, USA). 293 T cells were cultured in Dulbecco's modified Eagle's medium (DMEM, Gibco Life Technologies, Grand Island, NY, USA) containing 10% fetal bovine serum (HyClone, Logan, UT, USA). Cells were maintained in a humidified atmosphere at 37 °C with 5% CO_2. For the functional investigations, LECs were exposed to either normal glucose (NG, 5.56 mM) conditions or HG (25 mM) conditions for 24 h, according to a previous study[14].

Real-time polymerase chain reaction (Real-time PCR)

Total RNA in anterior lens capsule tissues or LECs was extracted using RNAsimple total RNA extraction kit (Tiangen Biotech Co. Ltd., Beijing, China). The yield of total RNA was determined using a NanoDrop 2000 spectrophotometer (Thermo Fisher Scientific Inc., Pittsburgh, PA, USA). Reverse-transcription PCR reaction was carried out in a reaction volume of 20 μL containing 1 μL oligo $(dT)_{15}$, 1 μL Random Primer Mix, 2 μL dNTP, 4 μL 5 × Buffer, 0.5 μL Rnase inhibitor, 1 μL M-MLV reverse transcriptase, 2 μg total RNA, and with ddH_2O supplementation. Reverse transcription conditions were 25 °C for 10 min, 42 °C for 50 min, followed by 80 °C for 10 min. Quantitative real-time PCR was conducted in a reaction volume of 20 μL containing 1 μL template cDNA, 0.5 μL PCR forward primer, 0.5 μL PCR reverse primer, 10 μL 2 × Taq PCR MasterMix, 0.5 μL SYBR GREEN, and with ddH_2O supplementation on an Exicycler™ 96 real-time quantitative thermocycler (Bioneer Corporation, Daejeon, Korea). The amplification condition was initial denaturation at 94 °C for 5 min, followed by 40 cycles of denaturation at 94 °C for 15 s and annealing at 60 °C for 20 s, extension at 72 °C for 30 s. Glyceraldehyde 3-phosphate dehydrogenase (GAPDH) or U6 small nuclear RNA (snRNA) were used as internal controls for mRNA or miRNA, respectively. Relative expression was calculated using the $2^{-\Delta\Delta CT}$ (CT indicated comparative threshold cycle) method. This experiment was repeated three times, and the specificity of each PCR was confirmed by melt curve analysis. The primers were self-designed using Primer Premier 5.0 software (Premier Tech Horticulture, Quebec, Canada). The sequences were: GAS5 (F: 5′-GGCTCTGGATAGCACCTT-3′, R: 5′-CTCCACCATTTCAACT TCC-3′); *TGFBR1* (F: 5′-GGTTCTGGCTCAGGTTTA-3′, R: 5′-TCTTTATTGTCTGCT GCTAT-3′); GAPDH (F: 5′-GACCTGACCTGCCGTCTAG-3′, R: 5′-AGGAGTGGGTG TCGCTGT-3′); hsa-miR-204-3p (F: 5′-GCTGGGAAGGCAAAGGGACGT-3′, R: 5′-GC AGGGTCCGAGGTATTC-3′); U6 (F: 5′-GCTTCGGCAGCACATATACT-3′, R: 5′-GC AGGGTCCGAGGTATTC-3′).

Cell infection

Short hairpin RNA (shRNA) targeting GAS5 (shRNA-GAS5), overexpression plasmid encoding *TGFBR1*, miR-204-3p mimic and inhibitor, and their vehicle controls (Wuhan JTS Scientific Co., Ltd., Wuhan, China) were cloned into the lentiviral vectors Tet-pLKO-puro (Addgene, Cambridge, MA, USA) or pLJM1-EGFP (Addgene). 293 T viral packaging cells were infected with recombinant lentiviral vectors to produce lentiviral particles. LECs grown approximately at a confluence of 70% received infection with lentiviral particles for 72 h at a multiplicity of infection (MOI) of 100. Real-time PCR was used to detect infection efficacy.

Scratch wound assay

After lentivirus infection, cells were scratched by a 200 μL sterile pipette tip in a straight line. Cells were then washed to remove debris and further cultured for 24 h. Images were taken with a light microscope (Olympus, Tokyo, Japan) at 0 h and 24 h after scratch.

Immunoblot analysis

Total protein in LECs was extracted using radio-immunoprecipitation assay (RIPA, Solarbio) lysis buffer containing 1 mM of phenylmethanesulfonyl fluoride (Solarbio). The yield of total protein was determined using a bicinchoninic acid (BCA) protein assay kit. An equal amount of protein (20 μg) was separated using sodium dodecyl sulfate-polyacrylamide gel electrophoresis (Solarbio) and then transferred onto polyvinylidene difluoride membranes (Millipore, Billerica, MA, USA). After blocking with 5% non-fat milk (Sangon Biotech Co., Ltd., Shanghai, China) or 5% bovine serum albumin (Biosharp life sciences, Hefei, China), the membranes were incubated with primary antibodies against Smad2 (AF6449, 1:1000 dilution, 52 kDa, Affinity Biosciences, Changzhou, China), activated (phosphorylated) Smad2 (p-Smad2, AF8314, 1:2000 dilution, 52 kDa, Affinity), vimentin (A19607, 1:1000 dilution, 54 kDa, ABclonal Biotechnology Co., Ltd., Wuhan, China), alpha-smooth muscle actin (a-SMA, AF1032, 1:2000 dilution, 42 kDa, Affinity), E-cadherin (A3044, 1:1000 dilution, 125 kDa, ABclonal) or GAPDH (60004-1-Ig, 1:10000 dilution, 36 kDa, Proteintech Group, Inc., Shanghai, China) at 4 °C overnight. Next, the membranes were incubated with horseradish peroxidase (HRP)-labeled goat anti-mouse (SE131, 1:3000 dilution, Solarbio) or HRP-labeled goat anti-rabbit (SE134, 1:3000 dilution, Solarbio). The blots were visualized using enhanced chemiluminescence (Solarbio).

Immunofluorescence

After lentivirus infection, cells were fixed with 4% paraformaldehyde (Sinopharm Chemical Regent Co., Ltd., Beijing, China) for 15 min and then permeabilized with 0.1% Triton X-100 (Beyotime Biotech Co., Ltd., Shanghai, China) for 30 min, blocked with goat serum (Solarbio) for 15 min, and incubated with primary antibodies against E-cadherin (A3044, 1:200 dilution, Abclonal), N-cadherin (66219-1-Ig, 1: 200 dilution, Proteintech), p-Smad2 (AP0548, 1: 200 dilution, Abclonal) and a-SMA (A17910, 1: 200 dilution, Abclonal) in a wet box at 4 °C overnight. On the following morning, cells were incubated with FITC-labeled anti-mouse antibody (ab6785, 1: 200 dilution, Abcam, MA, USA) and FITC-labeled anti-rabbit antibody (ab6717, 1: 200 dilution, Abcam), and cellular nuclei were

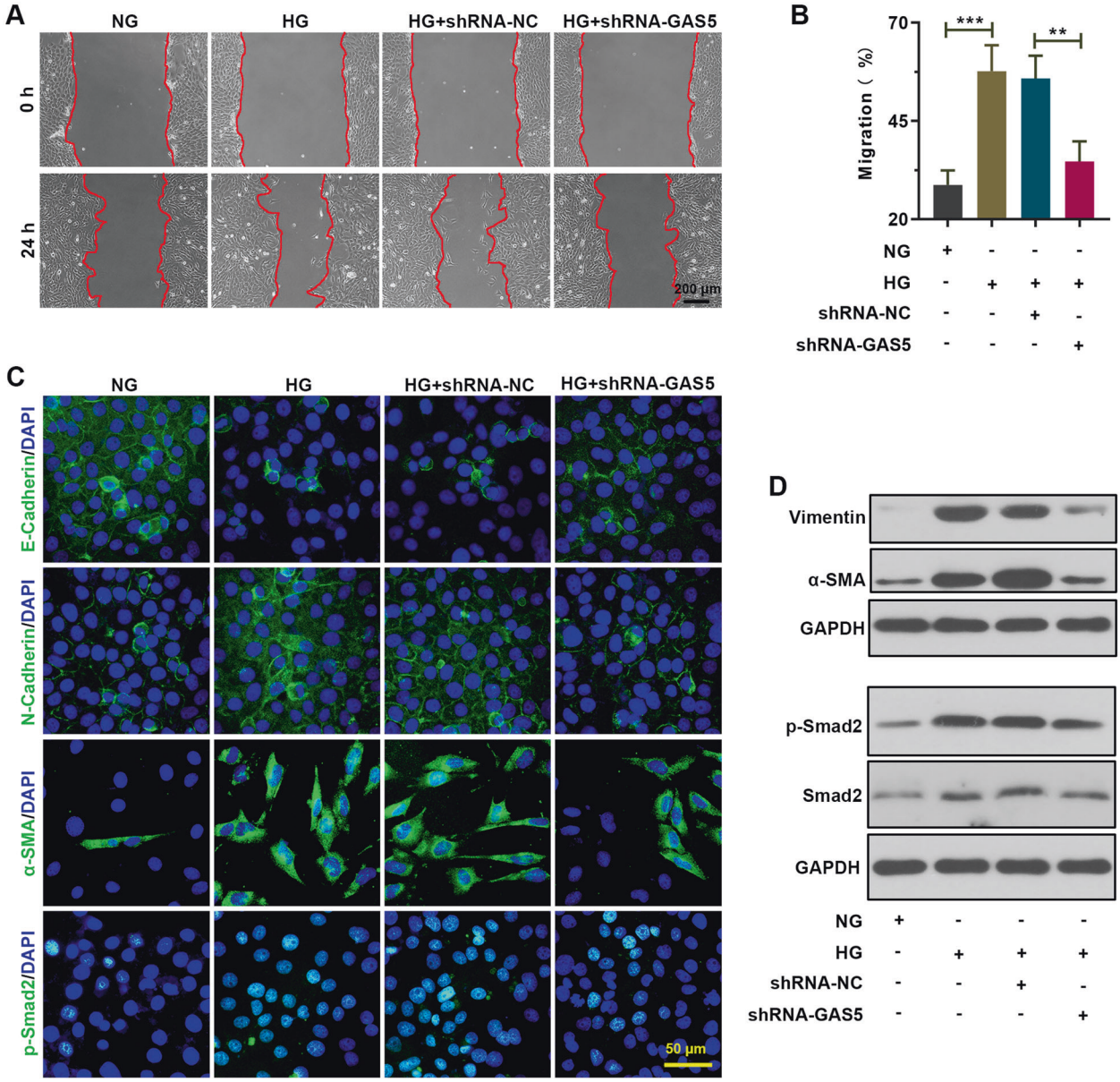

Fig. 2 Knockdown of lncRNA GAS5 inhibits migration and EMT in HG-treated LECs. A, B Cell migration was determined by scratch wound assay in NG or HG-treated LECs after infection of shRNA-NC or shRNA-GAS5. Scare bar, 200 μm ($n = 3$, each group). **C** The expression of E-cadherin, *N*-cadherin, *α*-SMA, and *p*-Smad2 was detected by immunofluorescence in NG or HG-treated LECs after infection of shRNA-NC or shRNA-GAS5. Scare bar, 50 μm ($n = 3$, each group). **D** The protein expression of vimentin, *α*-SMA, Smad2 and activated Smad2 (*p*-Smad2) was examined by immunoblot analysis in NG or HG-treated LECs after infection of shRNA-NC or shRNA-GAS5 ($n = 3$, each group). Data are presented as the mean ± SD ($n = 3$, each group). $^{**}P < 0.01$, $^{***}P < 0.001$, compared with NG group, or HG + shRNA-NC group.

counterstained with diamidino-2-phenylindole (DAPI, Beyotime). Cells were visualized using BX53 microscope (Olympus).

Dual-luciferase reporter gene assay

Biological prediction websites (LncBase V.2, TargetScanHuman 7.2, and miRDB) were employed to predict the binding sites of miR-204-3p and GAS5 or *TGFBR1* 3′UTR. The sequences of GAS5 with wild type (WT) or mutant (Mut) seed sites of miR-204-3p were cloned into the pmirGLO luciferase reporter vector (Nanjing Jinsirui Biotechnology Co., Ltd., Nanjing, China). The WT 3′-untranslated region (3′-UTR) sequence of *TGFBR1* containing miR-204-3p binding site or its Mut sequence was cloned into pmirGLO luciferase reporter vector. 293 T cells were co-infected with miR-negative control (miR-NC) or miR-204-3p mimic, and GAS5-WT, GAS5-Mut, *TGFBR1*-WT, or *TGFBR1*-Mut for 48 h. The fluorescence signals were detected using a luciferase detection kit on an M200pro multimode microplate reader (Tecan Group Ltd., Männedorf, Switzerland).

Statistical analysis

Statistical analysis was conducted using GraphPad Prism 8 software (GraphPad Software, Inc., La Jolla, CA, USA). The linear correlation between miR-204-3p and GAS5 or *TGFBR1* in DC tissues was calculated via Pearson correlation coefficient. The difference between the two groups was calculated via two-tailed Student's *t*-test. Difference among three or more groups was calculated via one-way ANOVA followed by Tukey's test. $P < 0.05$ was considered as statistically significant.

RESULTS

LncRNA GAS5 is up-regulated in DC tissues and HG-treated LECs

In the anterior lens capsule tissues from DC patients ($n = 30$), non-DC patients ($n = 30$), and human LECs treated with different concentrations of glucose, the expression level of lncRNA GAS5

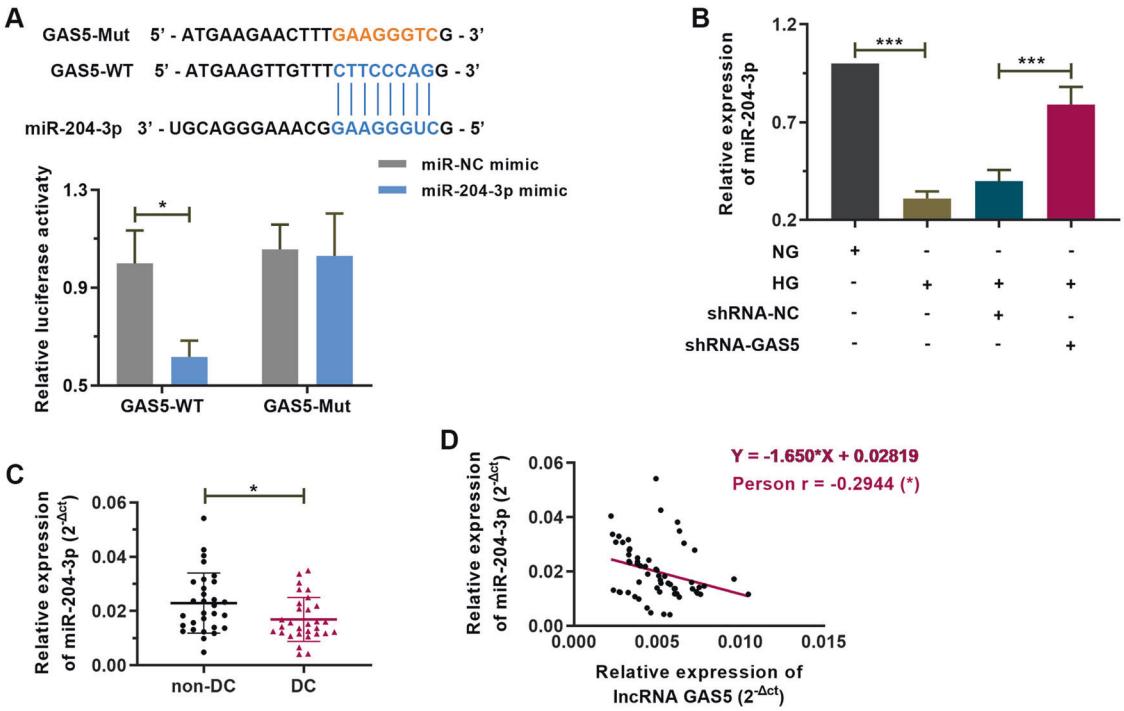

Fig. 3 MiR-204-3p is a target miRNA of lncRNA GAS5. A The binding sites of GAS5 and miR-204-3p were predicted by LncBase V.2. The luciferase activity was examined by dual-luciferase reporter gene assay in 293 T cells co-infected with GAS5-wild type (WT) or GAS5-mutant type (Mut) and miR-NC)mimic or miR-204-3p mimic ($n = 3$, each group). **B** The expression of miR-204-3p was detected using real-time PCR in NG or HG-treated LECs after infection of shRNA-NC or shRNA-GAS5 ($n = 3$, each group). **C** The expression of miR-204-3p was detected using real-time PCR in the anterior lens capsules of non-DC ($n = 30$) and DC ($n = 30$) patients. **D** Correlation between expression levels of lncRNA GAS5 and miR-204-3p. Data are presented as the mean ± SD. $^*P < 0.05$, $^{***}P < 0.001$, compared with non-DC group, NG group or miR-NC mimic group.

was detected using real-time PCR. The results showed that lncRNA GAS5 levels were up-regulated by 1.28-fold in DC tissues ($n = 30$) compared to non-DC tissues ($n = 30$) (Fig. 1A). GAS5 levels were increased by 4.82-fold in HG-treated LECs compared to NG-treated LECs (Fig. 1B).

Knockdown of GAS5 inhibits migration and EMT in HG-stimulated LECs

To investigate the functional role of GAS5 in DC, LECs were infected with lentivirus encoding shRNA-GAS5 to perform loss-of-function assays. Real-time PCR was applied to validate the infection efficiency (Supplementary Fig. 1A). Scratch wound assay, immunofluorescence, and immunoblot were then performed to monitor cell migration and EMT abilities. The results showed that HG treatment promoted LECs migration, whereas repression of GAS5 markedly inhibited their migration ability (Fig. 2A, B). Moreover, HG treatment notably reduced the expression of epithelial marker E-cadherin and increased the expression of mesenchymal markers vimentin, a-SMA, and N-cadherin in LECs. In contrast, depletion of GAS5 dramatically inhibited vimentin, a-SMA, and N-cadherin expression, while enhanced E-cadherin expression (Fig. 2C, D). Moreover, as the TGFβ/Smad signaling pathway is intensely associated with EMT in DC[27], the expression of a key protein in the pathway, p-Smad2, was examined. Repression of GAS5 markedly inhibited the HG-induced increase of p-Smad2 expression (Fig. 2C, D). Collectively, these data indicate that repression of GAS5 inhibited migration and EMT in HG-stimulated LECs.

MiR-204-3p is a target miRNA of GAS5

In order to investigate the role of GAS5 in migration and EMT of LECs, a miRNA that binds both GAS5 and *TGFBR1* 3′UTR was sought. Herein, the bioinformatics tools DIANA LncBase V.2[28], TargetScanHuman 7.2[29], and miRDB[30] were applied to analyze the target miRNAs of both GAS5 and *TGFBR1*. By searching the intersection of the three online databases, we found that 39 miRNAs might bind both GAS5 and *TGFBR1* 3′UTR. By investigating their functions through previous studies, we found that miR-204-3p has been reported to be down-regulated in cataract patients and was speculated to target 3′UTR of multiple oxidative stress-related genes[22], which gave us a hint that miR-204-3p dysregulation may be critical in triggering cataract progression.

To clarify the targeting relationship between GAS5 and miR-204-3p, a dual-luciferase reporter assay was performed. The results revealed that miR-204-3p mimic significantly decreased the luciferase activity of GAS5-WT, whereas it had no effect on that of GAS5-Mut (Fig. 3A). To further test their relationship, we analyzed miR-204-3p expression in clinical and cell samples. We observed that miR-204-3p expression was decreased in HG-treated LECs, whereas increased in HG-treated LECs intervened with lentivirus encoding shRNA-GAS5 (Fig. 3B). Moreover, in contrast to GAS5, expression of miR-204-3p was found significantly lowered in DC tissues (Fig. 3C). Pearson's correlation analysis revealed a negative correlation between GAS5 and miR-204-3p expression (Fig. 3D).

MiR-204-3p supplementation inhibits migration and EMT of HG-stimulated LECs

As the function of miR-204-3p in DC progression is also unclear, we further investigated the regulatory role of miR-204-3p in cell migration and EMT in DC. LECs were infected with lentivirus encoding miR-204-3p mimic to perform gain-of-function assays, and real-time PCR was performed to validate the infection efficiency. Expression of miR-204-3p expression was of over

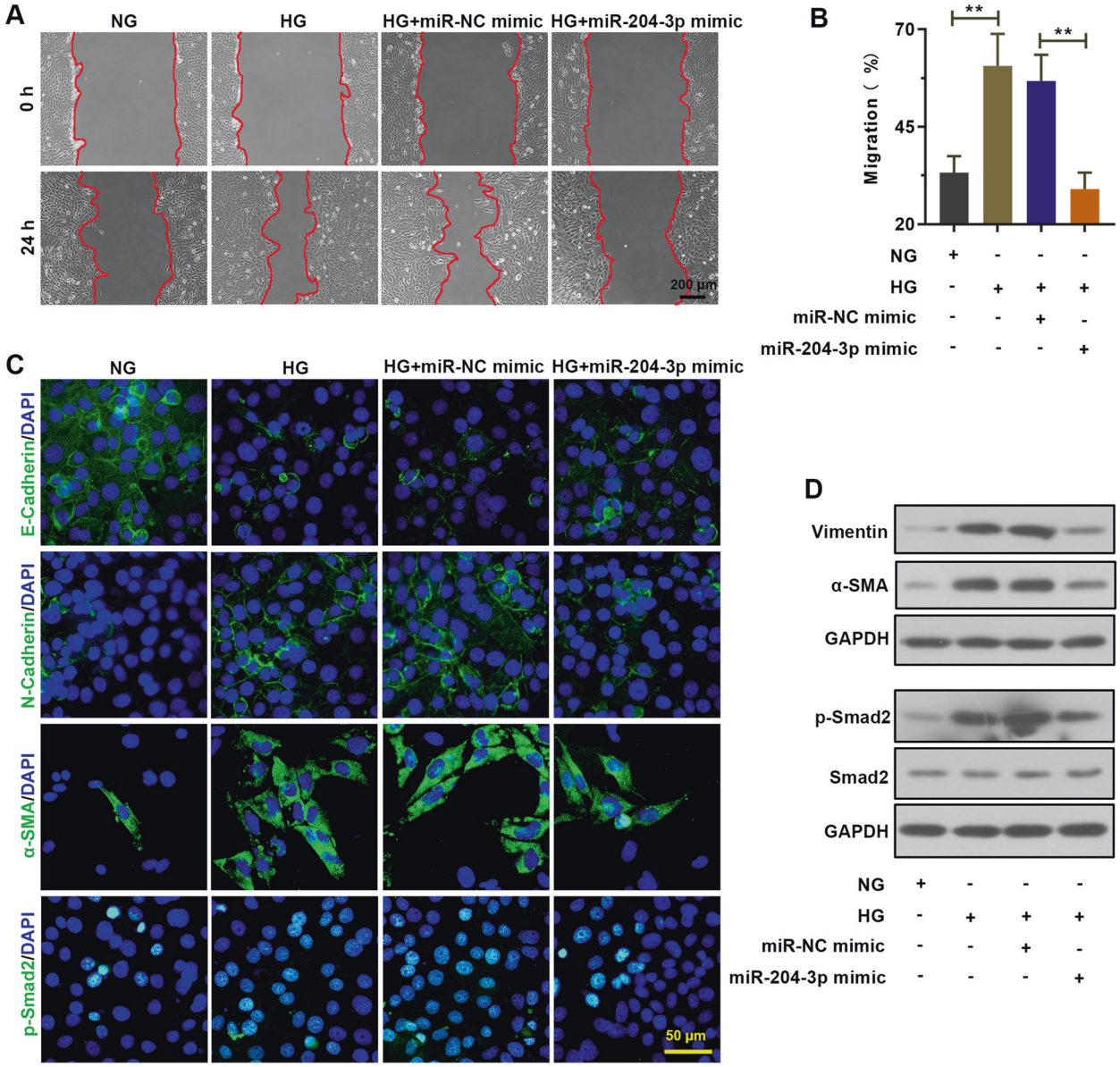

Fig. 4 MiR-204-3p inhibits migration and EMT in HG-treated LECs. A, B Cell migration was determined by scratch wound assay in NG or HG-treated LECs after infection of miR-NC mimic or miR-204-3p mimic. Scare bar, 200 μm ($n = 3$, each group). **C** The expression of E-cadherin, N-cadherin, α-SMA, and p-Smad2 was detected by immunofluorescence in NG or HG-treated LECs after infection of miR-NC mimic or miR-204-3p mimic. Scare bar, 50 μm ($n = 3$, each group). **D** The protein expression of vimentin, α-SMA, Smad2, and activated Smad2 (p-Smad2) was examined by immunoblot analysis in NG or HG-treated LECs after infection of miR-NC mimic or miR-204-3p mimic ($n = 3$, each group). $^{**}P < 0.01$, $^{***}P < 0.001$, compared with NG group, or HG + miR-NC mimic group.

8-fold increase after lentivirus infection (Supplementary Fig. 1B). Similar like GAS knockdown, miR-204-3p supplementation also showed suppressive effects on cell migration and EMT, along with a decrease of p-Smad2, vimentin, a-SMA and N-cadherin expression, and an increase of E-cadherin expression LECs (Fig. 4). These results indicate that miR-204-3p also had regulatory effects on LEC migration and EMT in DC.

MiR-204-3p deficiency reverses the effect of GAS5 knockdown on migration and EMT in HG-treated LECs

To further investigate whether GAS5 affects DC progression via modulating miR-204-3p, co-infection with lentiviruses encoding miR-204-3p inhibitor or shRNA-GAS5 was performed in HG-treated LECs. The results demonstrated that miR-204-3p inhibitor partially reversed the effect of GAS5 knockdown on the migration capacity, as well as the expression of epithelial marker E-cadherin and mesenchymal marker vimentin (Fig. 5), indicating that GAS5 affects migration and EMT in LECs by regulating miR-204-3p.

TGFBR1 is a target gene of miR-204-3p

TGFBR1 regulates the Smad pathway and EMT of LECs. The bioinformatics tools TargetScanHuman 7.2 and miRDB predicted binding sites of miR-204-3p and *TGFBR1* 3′UTR. To verify this finding, a dual-luciferase reporter gene assay was performed. Overexpression of miR-204-3p decreased the luciferase activity of *TGFBR1*-WT, but not the luciferase activity of *TGFBR1*-Mut (Fig. 6A). Additionally, the expression of *TGFBR1* was also found significantly up-regulated in DC tissues, which is in contrast with the expression of miR-204-3p (Fig. 6B). Pearson's correlation analysis also revealed a negative correlation between miR-204-3p and

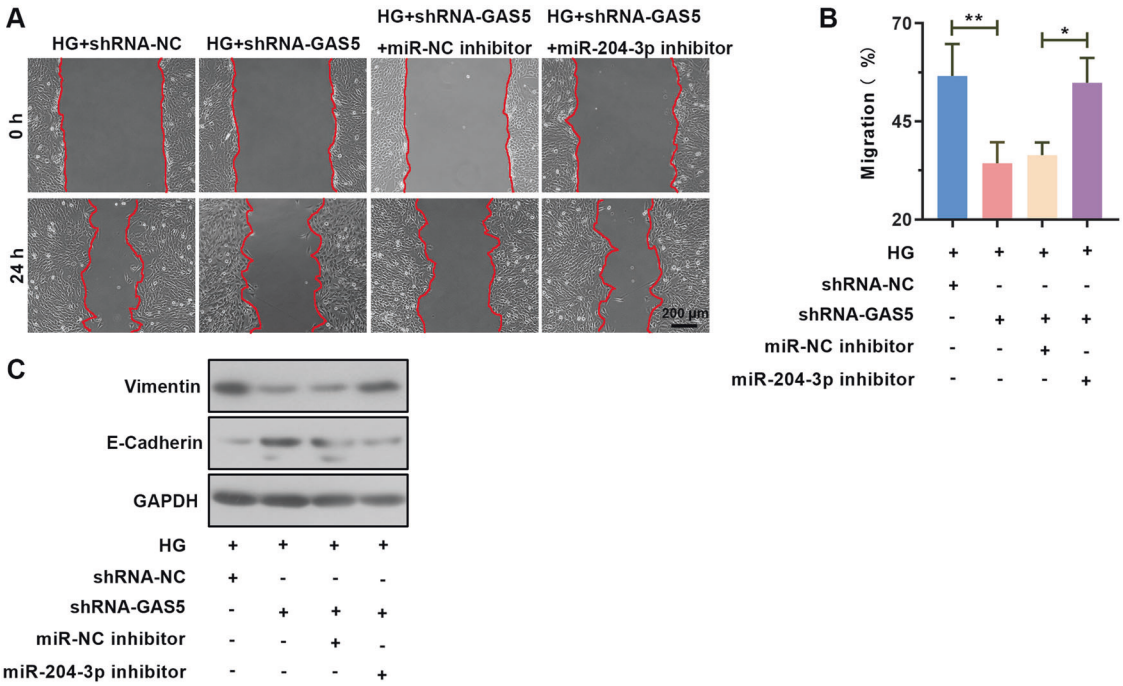

Fig. 5 MiR-204-3p deficiency reverses the effect of GAS5 knockdown on migration and EMT in HG-treated LECs. A, B Cell migration was determined by scratch wound assay in HG-treated LECs after co-infection of shRNA-NC or shRNA-GAS5 and miR-NC inhibitor or miR-204-3p inhibitor ($n = 3$, each group). Scare bar, 200 μm. **C** The protein expression of vimentin and E-cadherin was examined by immunoblot analysis in HG-treated LECs after co-infection of shRNA-NC or shRNA-GAS5 and miR-NC inhibitor or miR-204-3p inhibitor ($n = 3$, each group). $^{*}P < 0.05$, $^{**}P < 0.01$, $^{***}P < 0.001$, compared with HG + shRNA-NC group, or HG + shRNA-GAS5 + miR-NC inhibitor group.

TGFBR1 expression (Fig. 6C). Furthermore, in LECs stimulated by HG, expression of *TGFBR1* was found obviously up-regulated. Both miR-204-3p supplementation and GAS5 depletion showed inhibitory effects on *TGFBR1* expression, as shown by the results of immunoblot and immunofluorescence assays (Fig. 6D–G). These results indicated *TGFBR1* as a downstream target of miR-204-3p.

TGFBR1 overexpression reverses the effect of miR-204-3p on migration and EMT in HG-treated LECs

To investigate whether miR-204-3p affects DC progression via regulating *TGFBR1*, we co-transfected lentivirus encoding *TGFBR1* overexpression vector or miR-204-3p mimic into the HG-treated LECs. Infection efficiency was shown in Supplementary Fig. 1C. We demonstrated that *TGFBR1* overexpression reversed the effect of miR-204-3p on the expression of epithelial marker E-cadherin and mesenchymal marker vimentin (Fig. 7A). Furthermore, *TGFBR1* overexpression partially abolished the effect of miR-204-3p on migration (Fig. 7B–C). These findings show that miR-204-3p inhibits migration and EMT of HG-treated LECs by regulating *TGFBR1*.

DISCUSSION

Despite great advances in surgical technology for treating DC clinically, the incidences of surgical complications are relatively high. Screening of biomarkers has great guiding significance for discovering novel therapies for DC. It is generally believed that EMT of LECs is involved in the early pathogenesis of DC[8,10]. EMT is a critical physiological process that epithelial cells lose their polarized organization of the cytoskeleton to gain a motile mesenchymal phenotype and is associated with the loss of epithelial cell biomarkers and the obtainment of mesenchymal biomarkers[31,32]. Under HG conditions, LECs may obtain a mesenchymal phenotype with high migration capacity, which is pathogenetic for cataract progression[33]. Pharmacological or genetic inhibition of EMT of LECs has been verified to be effective in retarding DC progression[10]. However, the explicit molecular mechanism involved is largely unknown.

Recent studies have shown that lncRNAs have proved that they have critical regulatory roles in various processes, including the occurrence and development of DC[15,16,34]. In this work, we first describe that lncRNA GAS5 expression was significantly increased in DC tissues and in HG-stimulated LECs. LncRNA GAS5 is located on human chromosome 1q25.1 and participates in the regulation of various fundamental bioprocesses and disorders[35–37]. To investigate the function of GAS5 in DC progression, lentivirus encoding shRNA-GAS5 was infected into LECs, and EMT-related molecular changes were assessed. We observed that GAS5 silence effectively suppressed the migration of HG-stimulated LECs, which was associated with a reduction of mesenchymal biomarkers vimentin, a-SMA, and N-cadherin, but an increase of epithelial cell biomarker E-cadherin, indicating that knockdown of GAS5 inhibits HG-induced LEC migration and EMT.

In addition, numerous studies have highlighted that lncRNAs bind to miRNAs by acting as competing endogenous RNAs (ceRNAs), thereby influencing the expression of mRNAs and downstream target genes[38]. The correlation between lncRNAs, miRNAs, and mRNAs suggests a complicated regulatory mechanism in various diseases[13,39,40]. In this work, we confirmed that lncRNA GAS5 potentially binds to miR-204-3p. MiR-204-3p has been shown to contribute to the regulation of neurodegenerative disorders[41], familial Mediterranean fever[42], and certain types of cancer[43–45]. Han et al. revealed that miR-204-3p attenuated HG-induced apoptosis and dysfunction in podocytes[46]. Consistently, we demonstrated that miR-204-3p is down-regulated in DC samples and is also intensely associated with the regulation of migration and EMT in HG-cultured LECs. Moreover, we performed a rescue experiment to demonstrate that GAS5 influenced LEC migration and EMT by regulating miR-204-3p.

To further elucidate the molecular mechanisms that underlie the protective role of miR-204-3p on DC, we screened the target

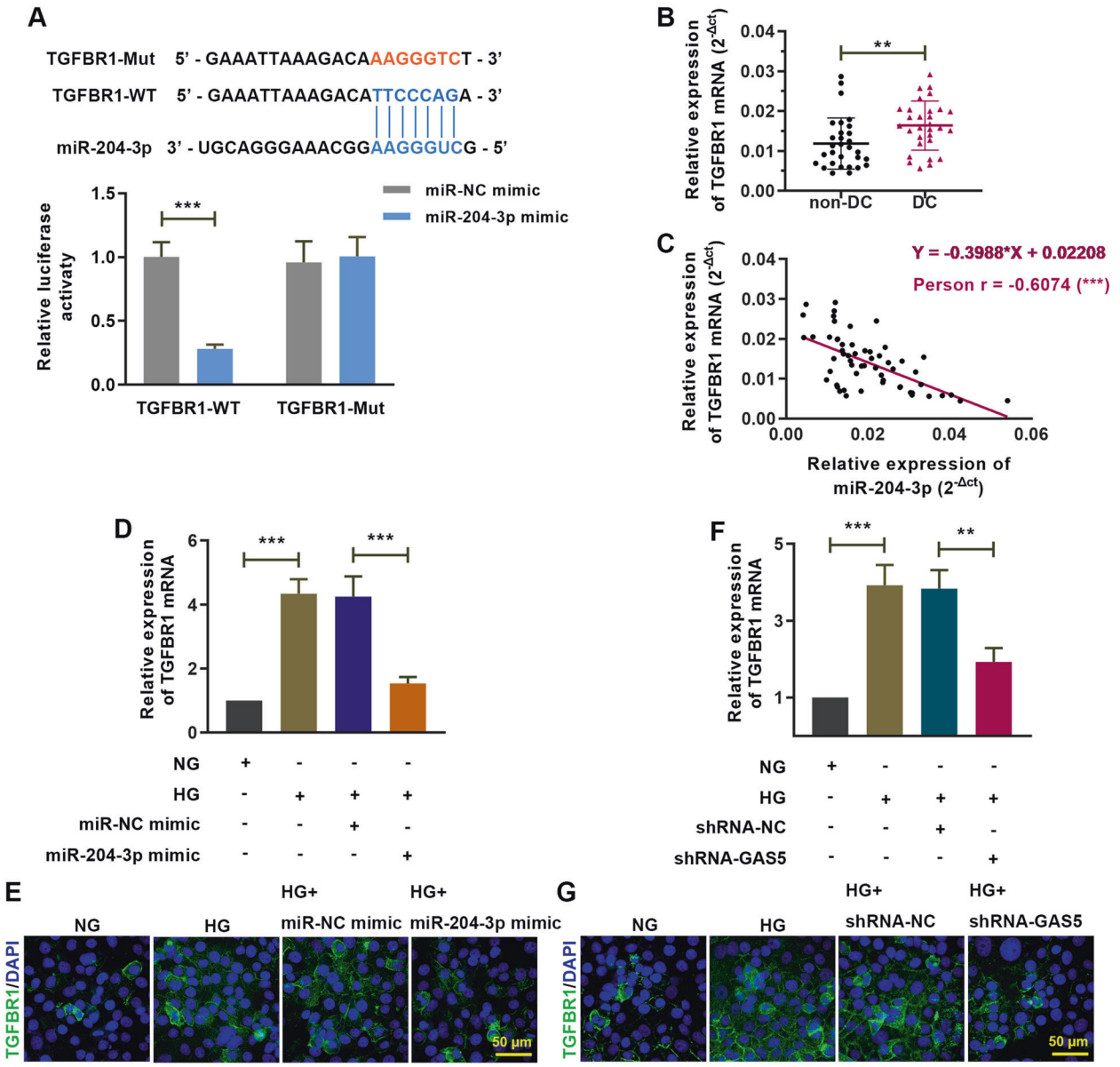

Fig. 6 ***TGFBR1* is a target gene of miR-204-3p. A** The binding sites of *TGFBR1* 3'UTR and miR-204-3p were predicted by TargetScanHuman 7.2 and miRDB. The luciferase activity was examined by dual-luciferase reporter gene assay in 293 T cells co-infected with *TGFBR1*-wild type (WT) or *TGFBR1*-mutant type (Mut) and miR-NC or miR-204-3p mimic ($n = 3$, each group). **B** The expression of *TGFBR1* mRNA was detected using real-time PCR in the anterior lens capsules of non-DC ($n = 30$) and DC ($n = 30$) patients. **C** Correlation between expression levels of miR-204-3p and *TGFBR1*. **D** The expression of TGFBR1 mRNA was detected using real-time PCR in NG or HG-treated LECs after infection of miR-NC mimic or miR-204-3p mimic ($n = 3$, each group). **E** The expression of TGFBR1 protein was detected using immunofluorescence in NG or HG-treated LECs after infection of miR-NC mimic or miR-204-3p mimic ($n = 3$, each group). **F** The expression of *TGFBR1* mRNA was detected using real-time PCR in NG or HG-treated LECs after infection of shRNA-NC or shRNA-GAS5 ($n = 3$, each group). **G** The expression of *TGFBR1* protein was detected using immunofluorescence in NG or HG-treated LECs after infection of shRNA-NC or shRNA-GAS5. Scare bar, 50 μm ($n = 3$, each group). $^{**}P < 0.01$, $^{***}P < 0.001$, compared with non-DC group, NG group or miR-NC mimic group.

genes of miR-204-3p and found that miR-204-3p potentially binds to *TGFBR1*. TGF-β1 performs a complex and important role in the initiation of the EMT process through a signal cascade that is activated when TGF-β1 attaches to *TGFBR1*, thereby stimulating the Smad signaling[26,47]. The activation process triggers the phosphorylation of Smad2 and Smad3 elements, thereby establishing a heterologous complex with Smad4 and then relocating to the nucleus to regulate the expression of target genes that related to EMT induction[48–50]. In this work, we found that both *TGFBR1* and p-Smad2 were up-regulated in HG-treated LECs. Intriguingly, we found not only miR-204-3p supplementation but also GAS5 depletion showed inhibitory effects on *TGFBR1* expression. Rescue experiments further confirmed that *TGFBR1* served as a downstream target of the GAS5/miR-204-3p axis.

The present study has some limitations. First, although the lncRNA-miRNA-mRNA network is a significant mechanism in the regulatory role of lncRNA GAS5, we cannot exclude the possibility that GAS5 may affect disease progression via other molecular mechanisms, such as lncRNA-protein interaction, chromatin remodeling, or histone modification. Second, like many other lncRNAs, GAS5 is also poorly conserved across mammalian species. It is very hard to further verify its function in vivo. Further in-depth investigations are clearly warranted.

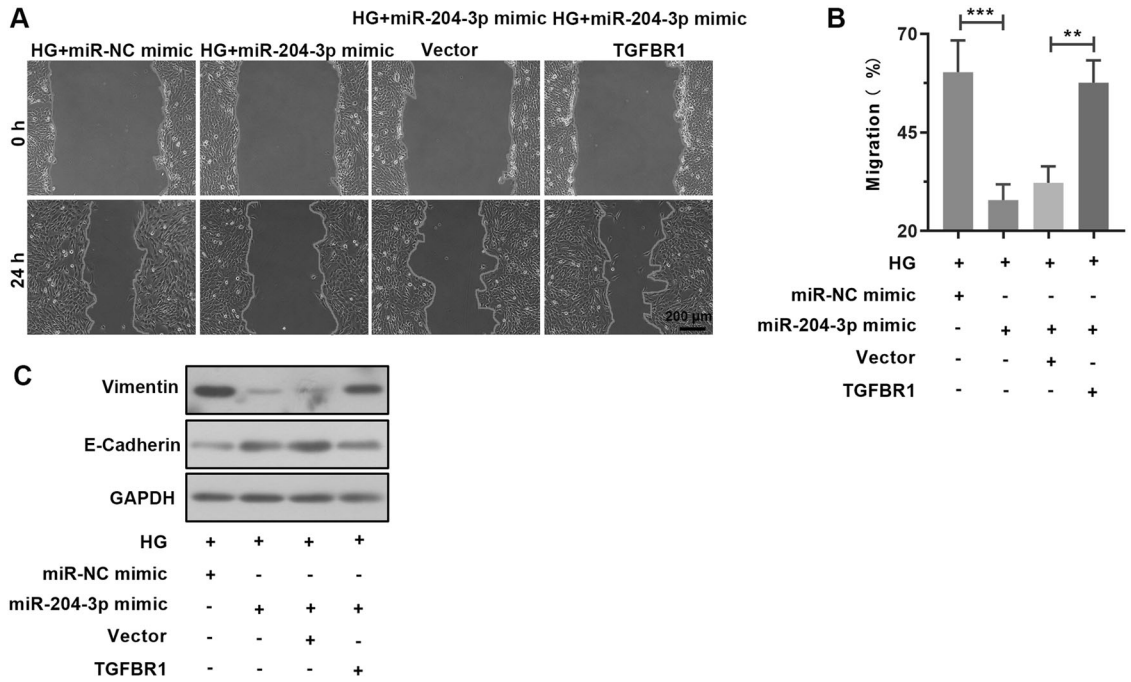

Fig. 7 *TGFBR1* overexpression reverses the effect of miR-204-3p on migration and EMT in HG-treated LECs. A, B Cell migration was determined by scratch wound assay in HG-treated LECs after co-infection of miR-NC mimic or miR-204-3p mimic and vector or *TGFBR1*-overexpression vector ($n = 3$, each group). Scare bar, 200 μm. **C** The protein expression of vimentin and E-cadherin was examined by immunoblot analysis in HG-treated LECs after co-infection of miR-NC mimic or miR-204-3p mimic and vector or *TGFBR1*-overexpression vector ($n = 3$, each group). $^{**}P < 0.01$, $^{***}P < 0.001$, compared with HG + miR-NC mimic group, or HG + miR-204-3p mimic + Vector group.

In summary, we demonstrated that repression of lncRNA GAS5 suppressed migration and EMT of HG-treated LECs by down-regulating miR-204-3p and subsequently up-regulating *TGFBR1*, thereby inactivating Smad2 phosphorylation. The network of GAS5/miR-204-3p/*TGFBR1* axis may provide new insights on the understanding of molecular mechanisms associated with DC.

DATA AVAILABILITY

The data that support the findings of this study are available from the corresponding author upon reasonable request.

REFERENCES

1. De Bruyne S., et al. A potential role for fructosamine-3-kinase in cataract treatment. *Int. J. Mol. Sci.* **22**, 3841 (2021).
2. Peterson, S. R., Silva, P. A., Murtha, T. J. & Sun, J. K. Cataract surgery in patients with diabetes: management strategies. *Semin. Ophthalmol.* **33**, 75–82 (2018).
3. Obrosova, I. G., Chung, S. S. & Kador, P. F. Diabetic cataracts: mechanisms and management. *Diabetes Metab. Res. Rev.* **26**, 172–180 (2010).
4. Šimunović, M. et al. Cataract as early ocular complication in children and adolescents with type 1 diabetes mellitus. *Int. J. Endocrinol.* **2018**, 6763586 (2018).
5. Hashim, Z. & Zarina, S. Advanced glycation end products in diabetic and non-diabetic human subjects suffering from cataract. *Age (Dordr)* **33**, 377–384 (2011).
6. Chancellor, J. et al. Intraoperative complications and visual outcomes of cataract surgery in diabetes mellitus: a multicenter database study. *Am. J. Ophthalmol.* **225**, 47–56 (2021).
7. Iyengar, L. & Lovicu, F. J. Aqueous humour-induced lens epithelial cell proliferation requires FGF-signalling. *Growth Factors* **35**, 131–143 (2017).
8. Li, J. et al. Activation of autophagy inhibits epithelial to mesenchymal transition process of human lens epithelial cells induced by high glucose conditions. *Cell Signal* **75**, 109768 (2020).
9. Liu, X. et al. microRNA-199a-5p regulates epithelial-to-mesenchymal transition in diabetic cataract by targeting SP1 gene. *Mol. Med.* **26**, 122 (2020).
10. Du, L. et al. Quercetin inhibited epithelial mesenchymal transition in diabetic rats, high-glucose-cultured lens, and SRA01/04 cells through transforming growth factor-β2/phosphoinositide 3-kinase/Akt pathway. *Mol. Cell Endocrinol.* **452**, 44–56 (2017).
11. Wu T. T., et al. AKR1B1-induced epithelial-mesenchymal transition mediated by RAGE-oxidative stress in diabetic cataract lens. *Antioxidants (Basel)* **9**, 273 (2020).
12. Mattick, J. S. The genetic signatures of noncoding RNAs. *PLoS Genet.* **5**, e1000459 (2009).
13. Huang, Y. The novel regulatory role of lncRNA-miRNA-mRNA axis in cardiovascular diseases. *J. Cell Mol. Med.* **22**, 5768–5775 (2018).
14. Gong, W., Zhu, G., Li, J. & Yang, X. LncRNA MALAT1 promotes the apoptosis and oxidative stress of human lens epithelial cells via p38MAPK pathway in diabetic cataract. *Diabetes Res. Clin. Pract.* **144**, 314–321 (2018).
15. Yang, J., Zhao, S. & Tian, F. SP1-mediated lncRNA PVT1 modulates the proliferation and apoptosis of lens epithelial cells in diabetic cataract via miR-214-3p/MMP2 axis. *J. Cell Mol. Med.* **24**, 554–561 (2020).
16. Li, Y., Jiang, S. H., Liu, S. & Wang, Q. Role of lncRNA NEAT1 mediated by YY1 in the development of diabetic cataract via targeting the microRNA-205-3p/MMP16 axis. *Eur. Rev. Med. Pharmacol. Sci.* **24**, 5863–5870 (2020).
17. Nguyen, L. N. T. et al. Long non-coding RNA GAS5 regulates T cell functions via miR21-mediated signaling in people living with HIV. *Front Immunol.* **12**, 601298 (2021).
18. Lv, L. et al. Silence of lncRNA GAS5 alleviates high glucose toxicity to human renal tubular epithelial HK-2 cells through regulation of miR-27a. *Artif Cells Nanomed. Biotechnol.* **47**, 2205–2212 (2019).
19. Zhou, R. R. et al. Silencing of GAS5 alleviates glaucoma in rat models by reducing retinal ganglion cell apoptosis. *Hum Gene Ther* **30**, 1505–1519 (2019).
20. Zeng K., Feng, Q. G., Lin, B. T., Ma, D. H. & Liu, C. M. Effects of microRNA-211 on proliferation and apoptosis of lens epithelial cells by targeting SIRT1 gene in diabetic cataract mice. *Biosci. Rep.* **37**, 695–708 (2017).
21. Yu, S. Y. et al. Knockdown of lncRNA AK139328 alleviates myocardial ischaemia/reperfusion injury in diabetic mice via modulating miR-204-3p and inhibiting autophagy. *J. Cell Mol. Med.* **22**, 4886–4898 (2018).
22. Wu, C. et al. MiRNAs regulate oxidative stress related genes via binding to the 3′ UTR and TATA-box regions: a new hypothesis for cataract pathogenesis. *BMC Ophthalmol.* **17**, 142 (2017).
23. Saika, S. et al. Transient adenoviral gene transfer of Smad7 prevents injury-induced epithelial-mesenchymal transition of lens epithelium in mice. *Lab Invest* **84**, 1259–1270 (2004).
24. Raghavan, C. T. et al. AGEs in human lens capsule promote the TGFβ2-mediated EMT of lens epithelial cells: implications for age-associated fibrosis. *Aging Cell* **15**, 465–476 (2016).

25. Kubo E., Shibata, T., Singh, D. P. & Sasaki, H. Roles of TGF β and FGF Signals in the Lens: tropomyosin regulation for posterior capsule opacity. *Int. J. Mol. Sci.* **19**, 3093–4004 (2018).
26. de Iongh, R. U., Wederell, E., Lovicu, F. J. & McAvoy, J. W. Transforming growth factor-beta-induced epithelial-mesenchymal transition in the lens: a model for cataract formation. *Cells Tissues Organs* **179**, 43–55 (2005).
27. Das, S. J., Wishart, T. F. L., Jandeleit-Dahm, K. & Lovicu, F. J. Nox4-mediated ROS production is involved, but not essential for TGFβ-induced lens EMT leading to cataract. *Exp. Eye Res.* **192**, 107918 (2020).
28. Paraskevopoulou, M. D. et al. DIANA-LncBase v2: indexing microRNA targets on non-coding transcripts. *Nucleic Acids Res.* **44**, D231–D238 (2016).
29. Riffo-Campos Á. L., Riquelme, I. & Brebi-Mieville, P. Tools for Sequence-Based miRNA Target Prediction: What to Choose? *Int. J. Mol. Sci.* **17**, 1987–2004 (2016).
30. Chen, Y. & Wang, X. miRDB: an online database for prediction of functional microRNA targets. *Nucleic Acids Res* **48**, D127–d131 (2020).
31. Skrypek, N., Goossens, S., De Smedt, E., Vandamme, N. & Berx, G. Epithelial-to-mesenchymal transition: epigenetic reprogramming driving cellular plasticity. *Trends Genet.* **33**, 943–959 (2017).
32. Serrano-Gomez, S. J., Maziveyi, M. & Alahari, S. K. Regulation of epithelial-mesenchymal transition through epigenetic and post-translational modifications. *Mol. Cancer* **15**, 18 (2016).
33. Li, X., Wang, F., Ren, M., Du, M. & Zhou, J. The effects of c-Src kinase on EMT signaling pathway in human lens epithelial cells associated with lens diseases. *BMC Ophthalmol.* **19**, 219 (2019).
34. Liu, J. et al. LncRNA KCNQ1OT1 knockdown inhibits viability, migration and epithelial-mesenchymal transition in human lens epithelial cells via miR-26a-5p/ITGAV/TGF-beta/Smad3 axis. *Exp. Eye Res.* **200**, 108251 (2020).
35. Sun, D. et al. LncRNA GAS5 inhibits microglial M2 polarization and exacerbates demyelination. *EMBO Rep.* **18**, 1801–1816 (2017).
36. Ni, W. et al. Long noncoding RNA GAS5 inhibits progression of colorectal cancer by interacting with and triggering YAP phosphorylation and degradation and is negatively regulated by the m(6)A reader YTHDF3. *Mol. Cancer.* **18**, 143 (2019).
37. Zhao, J. H., Wang, B., Wang, X. H. & Xu, C. W. Effect of lncRNA GAS5 on the apoptosis of neurons via the notch1 signaling pathway in rats with cerebral infarction. *Eur. Rev. Med. Pharmacol. Sci.* **23**, 10083–10091 (2019).
38. Zhou, R. S. et al. Integrated analysis of lncRNA-miRNA-mRNA ceRNA network in squamous cell carcinoma of tongue. *BMC Cancer* **19**, 779 (2019).
39. Tang, X. J., Wang, W. & Hann, S. S. Interactions among lncRNAs, miRNAs and mRNA in colorectal cancer. *Biochimie* **163**, 58–72 (2019).
40. Wang, J. Y. et al. Potential regulatory role of lncRNA-miRNA-mRNA axis in osteosarcoma. *Biomed. Pharmacother* **121**, 109627 (2020).
41. Tao W., et al. miR-204-3p/Nox4 mediates memory deficits in a mouse model of alzheimer's disease. *Mol Ther* https://doi.org/10.1016/j.ymthe.2020.09.006 (2020).
42. Koga, T. et al. MicroRNA-204-3p inhibits lipopolysaccharide-induced cytokines in familial Mediterranean fever via the phosphoinositide 3-kinase γ pathway. *Rheumatology (Oxford)* **57**, 718–726 (2018).
43. Xi, X. et al. MicroRNA-204-3p represses colon cancer cells proliferation, migration, and invasion by targeting HMGA2. *J. Cell Physiol.* **235**, 1330–1338 (2020).
44. Guo, J. et al. MiR-204-3p inhibited the proliferation of bladder cancer cells via modulating lactate dehydrogenase-mediated glycolysis. *Front Oncol.* **9**, 1242 (2019).
45. Yuan, D. et al. LncRNA-ATB promotes the tumorigenesis of ovarian cancer via targeting miR-204-3p. *Onco Targets Ther.* **13**, 573–583 (2020).
46. Han, X., Li, Q., Wang, C. & Li, Y. MicroRNA-204-3p attenuates high glucose-induced mpc5 podocytes apoptosis by targeting braykinin B2 receptor. *Exp. Clin. Endocrinol. Diabetes* **127**, 387–395 (2019).
47. Saika, S. et al. Smad3 signaling is required for epithelial-mesenchymal transition of lens epithelium after injury. *Am. J. Pathol.* **164**, 651–663 (2004).
48. Thiery, J. P., Acloque, H., Huang, R. Y. & Nieto, M. A. Epithelial-mesenchymal transitions in development and disease. *Cell* **139**, 871–890 (2009).
49. Ji, Y. et al. Paeoniflorin suppresses TGF-β mediated epithelial-mesenchymal transition in pulmonary fibrosis through a Smad-dependent pathway. *Acta Pharmacol. Sin.* **37**, 794–804 (2016).
50. Beshay, O. N. et al. Resveratrol reduces gentamicin-induced EMT in the kidney via inhibition of reactive oxygen species and involving TGF-β/Smad pathway. *Life Sci.* **258**, 118178 (2020).

AUTHOR CONTRIBUTIONS

X.L. and G.Z. conceived and designed the study; X.L., M.S. and A.C. performed experiments; X.L. and M.S. collected and analyzed the data; X.L. wrote the original manuscript. G.Z. revised the original manuscript. All authors have approved the final version of the paper.

FUNDING

This study was supported by grants from the National Natural Science Foundation of China (Grant No. 81970786 and 81670836), the Medical Science and Technology Project Jointly Built of Henan Province (Grant No. LHGJ20190196), and the Key Scientific Research Projects of Henan Colleges and Universities (Grant No. 20A320031).

COMPETING INTERESTS

The authors declare no competing interests.

ETHICS APPROVAL

The procedures involved in humen were carefully carried out in accordance with the principles of the Declaration of Helsinki and approved by the Ethics Committee of the First Affiliated Hospital of Zhengzhou University Committee.

ADDITIONAL INFORMATION

Supplementary information The online version contains supplementary material available at https://doi.org/10.1038/s41374-021-00713-3.

Correspondence and requests for materials should be addressed to Guangying Zheng.

Reprints and permission information is available at http://www.nature.com/reprints

Publisher's note Springer Nature remains neutral with regard to jurisdictional claims in published maps and institutional affiliations.